ResearchGate

See discussions, stats, and author profiles for this publication at: https://www.researchgate.net/publication/278790516

Use of Charged Nanoparticles in NMR-Based Metabolomics for Spectral Simplification and Improved Metabolite Identification

ARTICLE *in* ANALYTICAL CHEMISTRY · JUNE 2015

Impact Factor: 5.64 · DOI: 10.1021/acs.analchem.5b01142 · Source: PubMed

READS

44

5 AUTHORS, INCLUDING:

Bo Zhang

The Ohio State University

12 PUBLICATIONS **159** CITATIONS

SEE PROFILE

Available from: Bo Zhang
Retrieved on: 01 February 2016

analytical chemistry

Article

pubs.acs.org/ac

Use of Charged Nanoparticles in NMR-Based Metabolomics for Spectral Simplification and Improved Metabolite Identification

Bo Zhang,[†,§] Mouzhe Xie,[†,§] Lei Bruschweiler-Li,[†,‡] Kerem Bingol,[†] and Rafael Brüschweiler*[,†,‡]

[†]Department of Chemistry and Biochemistry, [‡]Campus Chemical Instrument Center, The Ohio State University, Columbus, Ohio 43210, United States

Supporting Information

ABSTRACT: Metabolomics aims at a complete characterization of all metabolites in biological samples in terms of both their identities and concentrations. Because changes of metabolites and their concentrations are a direct reflection of cellular activity, it allows for a better understanding of cellular processes and function to be obtained. Although NMR spectroscopy is routinely applied to complex biological mixtures without purification, overlapping NMR peaks often pose a challenge for the comprehensive and accurate identification of the underlying metabolites. To address this problem, we present a novel nanoparticle-based strategy that differentiates between metabolites based on their electric charge. By adding electrically charged silica nanoparticles to the solution NMR sample, metabolites of opposite charge bind to the nanoparticles and their NMR signals are weakened or entirely suppressed due to peak broadening caused by the slow rotational tumbling of the nanometer-sized nanoparticles. Comparison of the edited with the original spectrum significantly facilitates analysis and reduces ambiguities in the identification of metabolites. This method makes NMR directly sensitive to the detection of molecular charges at constant pH, as demonstrated here both for model mixtures and human urine. The simplicity of the approach should make it useful for a wide range of metabolomics applications.

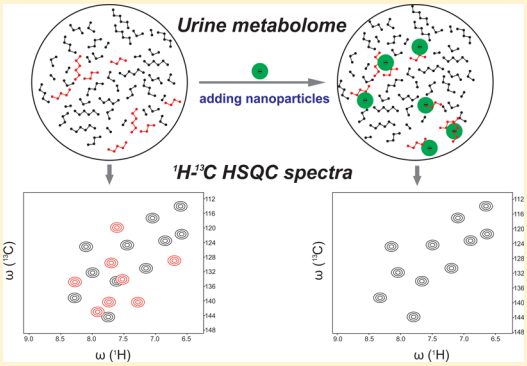

Over the past decade, metabolomics has made great progress in its quest to comprehensively study complex biological systems from a small molecule perspective.[1−3] Metabolomics focuses on the systematic characterization of individual components of the metabolome in biological systems at the levels of biofluids, cells, tissues, and whole organisms.[4−6] Identification and quantification the metabolites are important because they reflect a real-time snapshot of many cellular activities.[7]

NMR spectroscopy is one of two key experimental analysis methods in metabolomics due to its high spectral resolution, global detection capability, excellent reproducibility, and ease of sample preparation. However, depending on the complexity of the mixture, ambiguities in peak assignments and metabolite identities can exist in 1D and 2D NMR experiments.[8] Presently, one of the most powerful approaches for resolving such ambiguities relies on 2D TOCSY-type experiments,[9] which provide chemical connectivity information between multiple nuclear spins. This information can be used to deconvolute the NMR signals of individual metabolite components in complex mixtures.[10] Moreover, once individual mixture components have been deconvoluted, TOCSY spectra provide useful topology information toward their de novo structure elucidation.[11]

Targeted sample preparation approaches have been proposed to resolve peak ambiguities and to simplify the spectra in metabolomics applications. For example, the addition of paramagnetic ions, such as gadolinium and other lanthanides, can cause differential line broadening or the disappearance of peaks of certain metabolites through paramagnetic relaxation,[12] but such effects depend on a number of factors that are not easily predictable. Another approach specifically targets metabolites that contain carboxyl groups by having them react with ^{15}N cholamine isotope tags. The modified metabolites, which are detectable by ^{15}N NMR, can be identified provided that a customized NMR library of tagged metabolite products is available.[13]

Here, we present a strategy that monitors the modulation and disappearance of NMR signals of metabolites that strongly interact with electrically charged silica nanoparticles (SNPs). SNP colloid is directly mixed to the solution NMR metabolite sample, forming a stable, solution-like dispersion. Nanoparticles with diameters in the tens of nanometer range have very slow rotational tumbling correlation times in the microsecond range.[14] As a result, the tumbling rates of those metabolites that interact with the nanoparticles are slowed by several orders of magnitude in solution. This causes rapid transverse spin relaxation of these metabolites, which is manifested in dramatic line broadening and diminished peak amplitudes or complete

Received: March 25, 2015
Accepted: June 18, 2015
Published: June 18, 2015

ACS Publications © 2015 American Chemical Society

DOI: 10.1021/acs.analchem.5b01142
Anal. Chem. 2015, 87, 7211−7217

peak disappearance. Comparison of the NMR spectra of nanoparticle-free and -containing metabolite samples allows for the straightforward identification of NMR signals that belong to the subset of metabolites with opposite charge to the charge of the SNPs, facilitating the analysis of both 1D and 2D NMR spectra. We demonstrate the SNP-editing approach with both anionic and cationic SNPs.

EXPERIMENTAL SECTION

Chemicals and Materials. A pooled urine sample from healthy humans was obtained from (Innovative Research, Inc., Novi, MI). The following metabolites were obtained for the preparation of model mixtures: citric acid monohydrate ($C_6H_8O_7{\cdot}H_2O$, 99%), *N*,*N*-dimethylglycine ($C_4H_9O_2N$, 99%), D-glucose ($C_6H_{12}O_6$, 99.5%), L-glutamic acid ($C_5H_9NO_4$, 98.5%), L-histidine ($C_6H_9N_3O_2$, 98.5%), sodium lactate ($C_3H_5NaO_3$, 98%), sodium phosphate dibasic (Na_2HPO_4, 99.0%), sodium phosphate monobasic (NaH_2PO_4, 99.0%), and 3-(trimethylsilyl)-1-propanesulfonic acid sodium salt (DSS) were obtained from Sigma-Aldrich. L-Alanine ($C_3H_7NO_2$, 98.5%), L-arginine ($C_6H_{14}N_4O_2$, 98.5%), L-asparagine monohydrate ($C_4H_8N_2O_3{\cdot}H_2O$, 98.5%), L-glutamine ($C_5H_{10}N_2O_3$, 98.5%), L-lysine hydrochloride ($C_6H_{14}N_2O_2{\cdot}HCl$, 98.5%), and L-valine ($C_5H_{11}NO_2$, 98.5%) were purchased from Fisher BioReagents. Deuterium oxide (D_2O, 99.0%) was purchased from Cambridge Isotope Laboratory, Inc., Andover, MA. Amicon Ultra-15 Centrifugal Filter Units (3k and 10k NMWL) were purchased from Merck Millipore Ltd., Darmstadt, Germany.

Nanoparticle Preparation and Characterization. Bindzil 2040 silica nanoparticles (anionic SNPs) were obtained from Eka Chemicals. The surface of these SNPs is terminated by silanol (Si−OH) groups that experience partial deprotonation and lead to a negative charge under neutral pH conditions. Buffer exchange using a 10k NMWL Amicon filter unit was done for 1 mL of SNP colloid by repeatedly (at least 5 times) adding 10 mL of 20 mM sodium phosphate buffer, pH 7.0, dissolved in D_2O followed by centrifugation at 4300 rpm for 30 min to increase concentration. Finally, the volume of concentrated SNPs was adjusted back to 1 mL using the same phosphate buffer, with a recovery rate of 70%, and quantified by gravimetric analysis after complete solvent evaporation. The particle concentration was estimated to be 50 μM. LUDOX CL silica nanoparticles (cationic SNPs) were purchased from Sigma-Aldrich. According to the product's description, the surface of the particles is covered with a monolayer of alumina that results in a positive surface charge. Cationic SNP stock colloid (pH 4.0) was extensively dialyzed into 100 mM NaCl in H_2O, and the pH was adjusted to 5.5 using 0.5 M NaOH. The particle concentration was estimated to be 28 μM. The ζ-potentials of anionic and cationic SNPs were measured to be −23.0 ± 7.4 mV and +35.7 ± 6.9 mV (average ± standard deviation), respectively, using a Malvern Zetasizer Nano ZS at 25 °C (Figure 1 and Supporting Information).

Model Mixture Preparation. A model mixture of common metabolites consisting of unlabeled alanine, arginine, citric acid, dimethylglycine, glucose, histidine, lactic acid, lysine, shikimic acid, and valine with a uniform concentration of 2 mM was prepared in 20 mM sodium phosphate buffer at pH 7.0 in D_2O for experiments involving anionic SNPs. A 2-fold diluted model mixture (1 mM) in D_2O at pH 5.0 was used for cationic SNPs to maintain nanoparticle stability and prevent agglomeration.

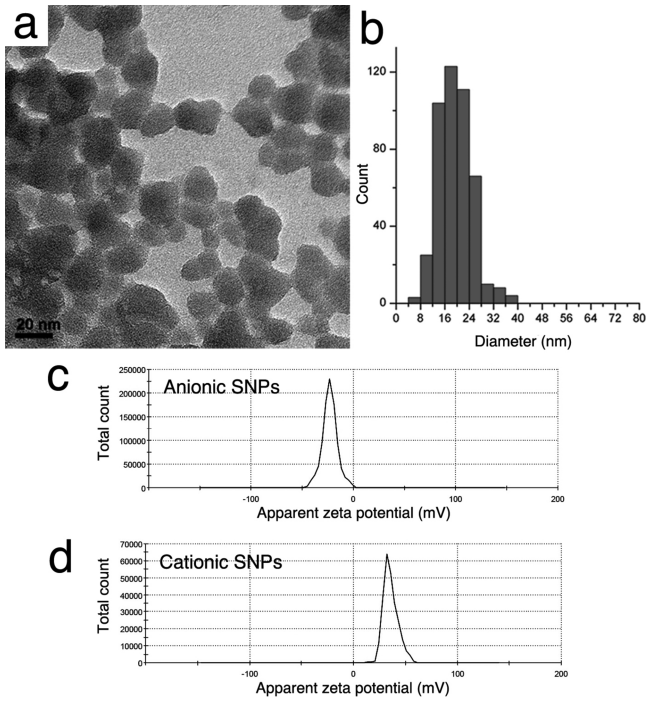

Figure 1. (a) TEM image and (b) size distribution of near-spherical anionic silica nanoparticles (SNPs) after being vacuum-dried and concentrated on a copper grid. Their size distribution was determined to be 19.5 ± 5.3 nm. ζ-potentials of (c) anionic SNPs at pH 5.5 and (d) cationic SNPs at pH 7.0 were measured to be −23.0 ± 7.4 mV and +35.7 ± 6.9 mV, respectively.

Protein Removal of Human Urine. One milliliter of the urine sample was thawed at 4 °C and filtered using a 3k NMWL Amicon filter unit at 4300 rpm for 20 min at 4 °C. The filter was washed twice with 2 mL of nanopure water each time, and all of the filtrates were pooled together before they were lyophilized and stored as a powder at −80 °C. The powder sample was dissolved in 1100 μL of 20 mM sodium phosphate buffer at pH 7.0. The nanoparticle-free sample was made of 550 μL of urine sample with 50 μL of phosphate buffer. The SNP-containing sample was made of 550 μL urine sample with 50 μL of anionic SNPs. Both samples also contained 100 μM DSS.

NMR Sample Preparation. Anionic and cationic SNPs (or pure buffer for control samples) were gently mixed with the reconstituted model mixture and/or urine metabolomics samples to a final volume of 600 μL before being placed in a 5 mm NMR tube for NMR data collection. The final particle concentration of anionic SNPs was estimated to be 8 μM for the model mixture and 4 μM for the urine sample, and approximately 4 μM cationic SNPs was used in the model mixture.

NMR Data Collection. All NMR spectra were collected on a Bruker AVANCE 850 MHz spectrometer equipped with a cryogenically cooled probe at 298 K. 1D ^{1}H NMR spectra of the model mixture were collected with 32 768 complex points at a 16 ppm spectral width with 64 scans (for anionic SNPs) to 256 scans (for cationic SNPs). 2D ^{13}C−^{1}H heteronuclear single quantum coherence (HSQC) spectra of the model mixture were collected with 512 × 1500 ($N_1 \times N_2$) complex points, 8012.820 Hz in the ^{1}H dimension and 32193.432 Hz in the ^{13}C dimension, with 16 scans (for anionic SNPs) or 32 scans (for cationic SNPs). 1024 and 3072 data points ($N_1 \times N_2$) were collected with 32 scans for the urine sample. The transmitter

DOI: 10.1021/acs.analchem.5b01142
Anal. Chem. 2015, 87, 7211−7217

frequency offsets were 4.70 and 80 ppm in the ^{1}H and ^{13}C dimensions, respectively.

NMR Data Analysis. All NMR data were zero-filled, Fourier transformed, and phase- and baseline-corrected. 1D ^{1}H NMR spectra were processed using the ACD/1D NMR manager, version 12.0 (Advanced Chemistry Development, Inc.). 2D NMR spectra were processed using NMRPipe.[15] To identify metabolites in the 1D and 2D NMR spectra, the COLMAR[16,17] databases were queried.

RESULTS

NMR Spectral Data of the Model Mixture. Ten compounds were chosen as a representative set of metabolites with different electrical charge properties (see Experimental Section). Figure 2 shows the 1D ^{1}H NMR and 2D $^{13}C-^{1}H$ HSQC spectra of the model mixture in the absence (left) and presence (right) of anionic SNPs. In the absence of SNPs, the 1D spectrum displays a certain level of peak overlap, which becomes resolved by the addition of SNPs. For example, arginine overlaps with other metabolites including lysine, histidine, glucose, and dimethyglycine. The addition of anionic SNPs leads to the removal of all arginine peaks, which simplifies the analysis and quantitation of the other metabolites. To quantify the effect of SNP addition, the average signal-to-noise ratios of all unique peaks of each metabolite were measured with and without SNPs, and their ratios (SNP free/SNP containing) were converted into a suppression factor (Table S1). The only positively charged metabolites, arginine, lysine, and histidine, rank as the top three compounds in terms of peak suppression. Since histidine has a side chain pK_a of 6.0 with a pI value of 7.59, at pH 7.0 it is only partially charged and hence it does not interact with the SNPs as strongly as does arginine or lysine, which is consistent with the results in Table S1. The model mixture also demonstrates that other compounds, such as valine, with local charges but zero net charge, can be partially suppressed as well. We observed that anionic SNPs have a tendency to interact with compounds containing clusters of hydrophobic methyl groups (dimethylglycine and valine). None of the negatively charged metabolites were perturbed by the addition of SNPs. The spectral simplification induced by the nanoparticles is also obvious in the 2D $^{13}C-^{1}H$ HSQC spectrum with the suppressed peaks marked by small rectangles (Figure 2). All cross-peaks of the positively charged metabolites are suppressed entirely beyond the detection limit, whereas the cross-peaks of the partially charged metabolites remain observable. The latter resonances do not show any noticeable chemical shift changes due to the addition of the nanoparticles, provided that the pH is not changed. Only very weak line broadening is observed for the noninteracting metabolites, which might be due to a slight increase in the overall viscosity of the mixture leading to somewhat slower rotational tumbling behavior.

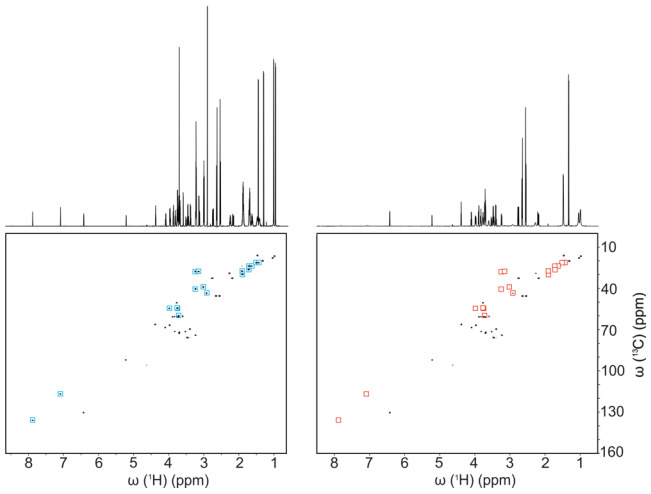

Figure 2. 1D ^{1}H and 2D $^{13}C-^{1}H$ HSQC spectra of 10-compound model mixture (a) without and (b) with anionic SNPs. Red and blue squares highlight the cross-peaks that are suppressed by the presence of SNPs.

NNR Spectral Data of the Urine Sample. Human urine has served in metabolomics studies as an archetype among biofluids. It has been used for biomarker identification,[18] disease classification[19] and drug toxicity evaluation.[20] It was chosen here because of its challenging metabolome that displays a high level of complexity. Our COLMAR $^{13}C-^{1}H$ HSQC web server[21] was used for automatic peak assignment.[16] The spectrum of SNP-free urine sample was compared to the one with anionic SNPs added, highlighting those cross-peaks stemming from compounds that were suppressed by the presence of nanoparticles (Tables 1, 2). Three representative spectral regions that show the spectral changes induced by the SNPs are depicted in Figure 3. The peak assignments of these metabolites were independently verified using $^{13}C-^{1}H$ TOCSY–HSQC and $^{1}H-^{1}H$ TOCSY NMR spectra.[22] Three

Table 1. List of Metabolites with Attenuated Peaks in Anionic SNP-Containing Urine Sample

NP suppressed	charge	nitrogen no.
1-methylhistidine	0	1
1-methylguanidine	1	3
betaine	0	1
carnitine	0	1
creatinine	0	3
dimethylamine	1	1
dimethylglycine	0	1
lysine	1	2
trigonelline	0	1
trimethylamine *N*-oxide	0	1

Table 2. Effect of Anionic SNPs on Detection of Amino Acids in Human Urine Sample[a]

amino acid	charge	suppressed
alanine	0	no
arginine	+1	yes
asparagine	0	no
aspartic acid	−1	no
glutamic acid	−1	no
glutamine	0	no
glycine	0	no
lysine	+1	yes
serine	0	no
threonine	0	no
tyrosine	0	no
valine	0	no

[a]Metabolites whose NMR spectrum was suppressed by SNPs in the urine sample. Other amino acids were either not present or below the detection limit.

DOI: 10.1021/acs.analchem.5b01142
Anal. Chem. 2015, 87, 7211−7217

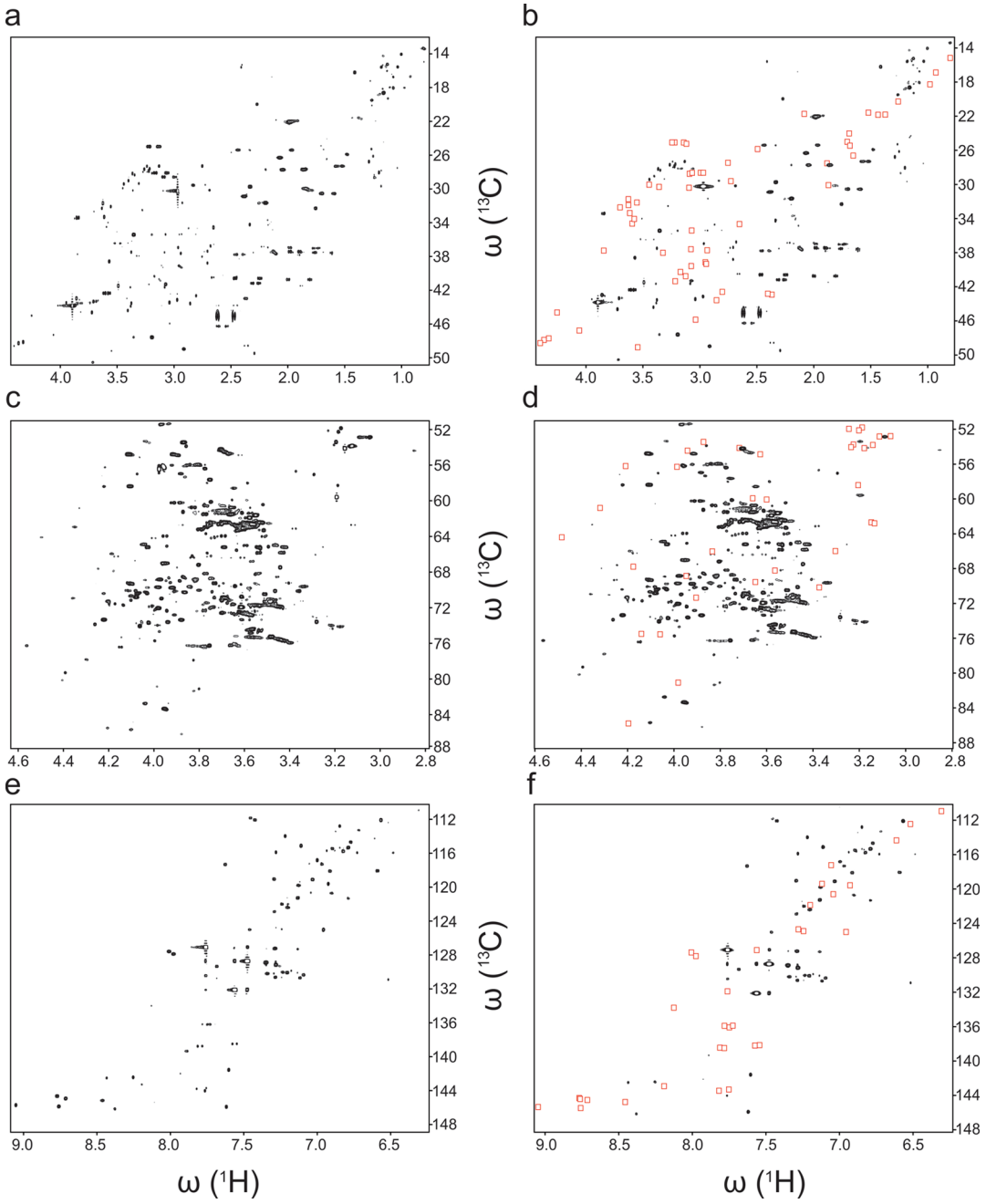

Figure 3. Effect of anionic SNPs on 2D $^{13}C-^{1}H$ HSQC NMR spectrum of human urine sample. Three representative spectral regions demonstrate the cross-peak suppression by SNP addition. Red boxes indicate missing cross-peaks in the spectrum (a, c, e) without and (b, d, f) with SNPs.

of these metabolites are positively charged, three of them have no net charge and possess tertiary amine groups, and the other four metabolites possess a quaternary ammonium group. Negatively charged acidic metabolites, such as lactic acid, citric acid, and acetic acid, were not perturbed. Zwitterions, such as amino acids, were suppressed only when they have a net positive charge. Many of the metabolites observed in the human urine 2D $^{13}C-^{1}H$ HSQC spectrum were observed in previous urine NMR metabolomics studies.[23] Metabolites that have only one or two cross-peaks, such as methylguanidine or dimethylglycine, can be easily misassigned due to peak overlaps. Therefore, their SNP-based identification on the basis of their positive charge helps to identify them unambiguously. As for the model mixture, no noticeable chemical shift changes were observed when the SNPs were added.

DISCUSSION

A New Direction To Probe Metabolite Properties Using Nanoparticles. It has been reported that uncharged hydrophobic metabolites have a lower concentration in living cells due to their lower solubility and higher chance of leakage out of the membrane. Studying charged metabolites can potentially contribute to a better understanding of metabolic homeostasis.[24] NMR spectroscopy is exquisitely sensitive to local magnetic fields reflected in chemical shifts, but it is much less sensitive to electric charges (pH titration experiments represent a notable exception).[25] An electrophoretic NMR

DOI: 10.1021/acs.analchem.5b01142
Anal. Chem. 2015, 87, 7211−7217

technique has been proposed that focuses on the charge properties of molecules using a specially designed NMR apparatus.[26,27] However, for complex biological mixtures with hundreds of small molecules, this approach does not provide the necessary resolution. Therefore, existing charge information about molecules of interest cannot be easily used for the interpretation of NMR spectra of complex mixtures at constant pH.

With the introduction of charged nanoparticles described in this work, the net charge of metabolites is directly reflected in the NMR spectra through the appearance and disappearance of NMR cross-peaks. Differentiation between metabolites based on their electric charge is possible if the following two conditions are fulfilled: (1) SNP-bound metabolites are restricted in their rotational Brownian diffusion, causing the quenching of their NMR signals, and (2) the nanoparticles neither contribute to the NMR spectrum nor perturb the NMR peaks of molecules that do not interact with them. The SNP-based strategy presented here does not require new or modified hardware.

Interactions between Nanoparticles and Metabolites in a Biological System. Progress in nanoparticle research shows promise in many different areas, including biomedical imaging and disease diagnosis and treatment, such as targeted magnetic resonance imaging (MRI),[28] photoacoustic imaging,[29] point-of-care diagnosis using a lab-on-a-chip,[30] drug delivery,[31] and photobased physical therapy.[32] However, the toxicity of nanoparticles has always been a practical concern, and its impact on nucleic acids,[33,34] proteins,[35,36] or even intact cells[37,38] has been discussed. Yet, very little is known about the effects of metabolome−nanoparticle interactions. In this work, the presence of specific interactions between nanoparticles and certain types of metabolites was established for human urine by NMR. Considering the abundance of many of these metabolites in other biofluids and biological systems, it is likely that, in these systems, SNPs interact with metabolites in the same way. The fact that changes in the pattern of the metabolome can modulate and disrupt biological pathways and biomolecular activities suggests that such effects might be relevant for toxicity evaluation of biomedical applications of nanomaterials. Conversely, the interaction of nanoparticles with charged small molecules could be used to detoxify and purify biological as well as artificial chemical mixtures.

In the present work, anionic SNPs were used whose silanol (Si−OH) groups on the surface are partially deprotonated at neutral pH, leading to a negative net charge,[39] which is stabilized by the presence of counterions. Two categories of metabolites were found here to have a strong tendency to bind to anionic SNPs (Tables 1, 2). The first category consists of metabolites with a net positive charge that experience an attractive electrostatic interaction to the negatively charged SNPs. The positively charged metabolites often contain a neutral basic group, which, after proton acceptance, becomes positively charged. Examples include lysine, arginine, and histidine, whose NMR peaks became suppressed after binding to the much larger nanoparticles. In addition, metabolites with a quaternary nitrogen that has a positive charge also belong to this category, such as choline, betaine, and trigonelline. The second category consists of metabolites that are neutral but that have multiple methyl groups. In particular, those molecules with multiple methyl groups that are connected to tertiary amine group have a relatively strong tendency to bind to SNPs. Similar observations were made for single-stranded DNA bound to negatively charged nanoparticles where the nitrogen atoms of each nucleotide were proposed to be the binding sites.[40] The addition of charged nanoparticles to an NMR sample can be likened to the conversion of the NMR sample into an affinity column analogous to solid-phase extraction, wherein the resins are micro- or nanosized silica particles. We focused on silica nanoparticles in this work, but quantum dots or other nanoparticles, such as gold- or silver-based nanoparticles, are likely to work as well.

To test whether our approach also works with an opposite role of charges, namely, with cationic SNPs interacting with anionic metabolites, cationic SNPs were added to the model mixture. As can be seen in Figure 4, the NMR signals of the

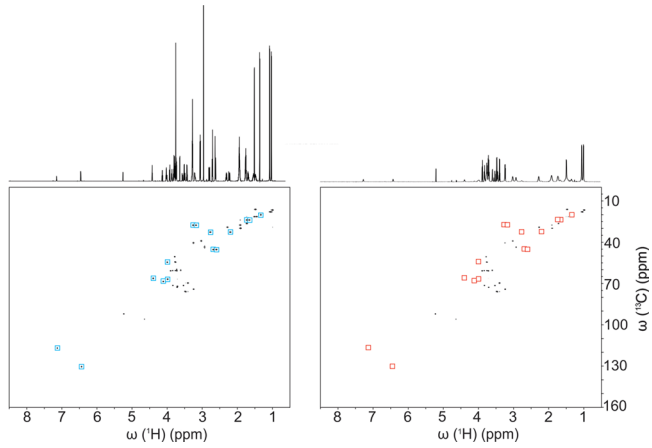

Figure 4. 2D $^{13}C-^{1}H$ HSQC spectra of 10-compound model mixture (a) without and (b) with cationic SNPs. Red and blue squares highlight the cross-peaks that are suppressed by the presence of SNPs.

negatively charged metabolites of the mixture, namely, citric acid, lactic acid, and shikimic acid, were either entirely suppressed or strongly weakened (less than 5% peak intensity left). Noncharged metabolites showed some line-broadening effects, similar to that in the anionic SNP case, which might be due to a moderate increase in the overall viscosity of the SNP solution.

The Challenge of Spectral Interpretation in NMR-Based Metabolomics. NMR-based metabolomics studies benefit from the possibility of conducting metabolomics studies with little or no separation prior to doing the NMR experiments. Such an untargeted approach allows one to keep the metabolome as intact as possible, which is important for many studies. On the downside, the resulting NMR spectra, especially 1D spectra, can be overcrowded so that peak identification becomes notably difficult. The 2D $^{13}C-^{1}H$ HSQC experiment belongs to the most popular approaches in 2D NMR-based metabolomics because the cross-peaks are greatly dispersed along the second dimension. Nevertheless, spectral regions can still exist with significant spectral overlap. For example, in region c of Figure 3, many peaks are so close to each other that they cannot be discriminated. However, the presence of cationic SNPs causes the disappearance of a subset of cross-peaks, significantly facilitating the analysis of those that remain. Since the $^{13}C-^{1}H$ HSQC spectrum does not provide information regarding which cross-peaks belong to the same molecule, it is possible that two cross-peaks that belong to two different metabolites, not contained in NMR databases, are assigned to a single metabolite in the databases that happens to

DOI: 10.1021/acs.analchem.5b01142
Anal. Chem. 2015, 87, 7211−7217

have two cross-peaks at approximately the same positions. Since the interaction of a metabolite with SNPs leads to the removal of all cross-peaks belonging to the metabolite, the disappearance of only one of the two cross-peaks implies that the two cross-peaks cannot belong to the same metabolite. In this way, the addition of SNPs can disambiguate tentative peak assignments in both 1D and 2D NMR spectra. For example, the NMR peaks of arginine are often very close to or overlap with those of other metabolites of a complex mixture. When querying the spectrum against the database, arginine could not be identified. By contrast, when querying only the subgroup of peaks that were suppressed in the presence of the SNPs, arginine could be identified with a matching ratio of 0.8 and a uniqueness of 3/5 (one of the broad multiplets of a CH_2 group was too weak to observe). On the other hand, metabolites that were identified based on the complete cross-peak list of the SNP-free sample, but not based on the two complementary groups of cross-peaks (suppressed vs unaltered), might be affected by false positive hits requiring further analysis.

CONCLUSIONS

Metabolomics is a research field where nanomaterials have yet to make a significant impact. Here, we introduced a strategy for NMR-based metabolomics by the selective, charge-based editing of the NMR spectra of the metabolites through the addition of charged nanoparticles. This represents a fast, easy, and cost-effective alternative to other metabolite separation approaches. It allows one to highlight a subset of metabolites in a complex mixture depending on molecular properties, including their net charge. Specifically, combining the NMR results from a nanoparticle-free sample, a sample with anionic nanoparticles, and one with cationic nanoparticles permits the unambiguous distinction and identification of neutral, negatively charged, and positively charged metabolites.

The approach presented here, bridging metabolomics with nanoscience, provides benefits on different levels. Traditionally, NMR has not been considered to be a sensitive detector of molecular electric charges, but the present application demonstrates how such information can be readily obtained. Additionally, NMR-based metabolomics has been limited by ambiguous peak assignments. With the help of charged nanoparticles, complicated NMR spectra, such as ones from urine samples, become simpler, promising their more accurate and efficient interpretation. Last but not the least, this study also casts light on the possibility of heterogeneous interactions between metabolites and nanoparticles in living organisms by changing the composition of the metabolome with potential implications for biological function. We expect that the nanoparticle-based editing approach will prove to be useful for the analysis of a wide range of complex mixtures in metabolomics and elsewhere.

ASSOCIATED CONTENT

Supporting Information

Additional information regarding the SNP measurements and properties (TEM, ζ-potential, DLS); 1D ^{1}H NMR spectra of independently prepared replicate samples with quantitative analysis. The Supporting Information is available free of charge on the ACS Publications website at DOI: 10.1021/acs.analchem.5b01142.

AUTHOR INFORMATION

Corresponding Author

*E-mail: bruschweiler.1@osu.edu.

Author Contributions

§B.Z. and M.X. contributed equally to this work.

Notes

The authors declare no competing financial interest.

ACKNOWLEDGMENTS

We thank Eka Chemicals for a generous gift of the anionic silica nanoparticles. This work was supported by the National Institutes of Health (grant no. R01 GM 066041 and SECIM grant no. U24 DK097209-01A1).

REFERENCES

(1) Nicholson, J. K.; Lindon, J. C. *Nature* **2008**, *455*, 1054−1056.
(2) Fiehn, O. *Plant Mol. Biol.* **2002**, *48*, 155−171.
(3) Bingol, K.; Brüschweiler, R. *Anal. Chem.* **2014**, *86*, 47−57.
(4) Tang, J. *Curr. Genomics* **2011**, *12*, 391−403.
(5) Zhang, A.; Sun, H.; Wang, P.; Han, Y.; Wang, X. *J. Proteomics* **2012**, *75*, 1079−1088.
(6) Wu, H.; Southam, A. D.; Hines, A.; Viant, M. R. *Anal. Biochem.* **2008**, *372*, 204−212.
(7) Halouska, S.; Fenton, R. J.; Barletta, R. G.; Powers, R. *ACS Chem. Biol.* **2012**, *7*, 166−171.
(8) Bingol, K.; Bruschweiler-Li, L.; Li, D.-W.; Brüschweiler, R. *Anal. Chem.* **2014**, *86*, 5494−5501.
(9) Braunschweiler, L.; Ernst, R. R. *J. Magn. Reson.* **1983**, *53*, 521−528.
(10) Bingol, K.; Brüschweiler, R. *Anal. Chem.* **2011**, *83*, 7412−7417.
(11) Bingol, K.; Zhang, F.; Bruschweiler-Li, L.; Brüschweiler, R. *J. Am. Chem. Soc.* **2012**, *134*, 9006−9011.
(12) Correa, J.; Pinto, L. F.; Riguera, R.; Fernandez-Megia, E. *Anal. Chem.* **2015**, *87*, 760−767.
(13) Tayyari, F.; Nagana Gowda, G. A.; Gu, H.; Raftery, D. *Anal. Chem.* **2013**, *85*, 8715−8721.
(14) Bloembergen, N.; Purcell, E. M.; Pound, R. V. *Phys. Rev.* **1948**, *73*, 679−712.
(15) Delaglio, F.; Grzesiek, S.; Vuister, G. W.; Zhu, G.; Pfeifer, J.; Bax, A. *J. Biomol. NMR* **1995**, *6*, 277−293.
(16) Zhang, F.; Robinette, S. L.; Bruschweiler-Li, L.; Brüschweiler, R. *Magn. Reson. Chem.* **2009**, *47*, S118−122.
(17) Bingol, K.; Zhang, F.; Bruschweiler-Li, L.; Brüschweiler, R. *Anal. Chem.* **2012**, *84*, 9395−9401.
(18) Ganti, S.; Weiss, R. H. *Urol. Oncol.* **2011**, *29*, 551−557.
(19) Kim, Y.; Koo, I.; Jung, B. H.; Chung, B. C.; Lee, D. *BMC Bioinf.* **2010**, *11*, S4.
(20) Zhang, Y.; Zhao, F.; Deng, Y.; Zhao, Y.; Ren, H. *J. Proteome Res.* **2015**, *14*, 1752−1761.
(21) Bingol, K.; Li, D.-W.; Bruschweiler-Li, L.; Cabrera, O. A.; Megraw, T.; Zhang, F.; Brüschweiler, R. *ACS Chem. Biol.* **2015**, *10*, 452−459.
(22) Bingol, K.; Brüschweiler, R. *J. Proteome Res.* **2015**, *14*, 2642−2648.
(23) Bouatra, S.; Aziat, F.; Mandal, R.; Guo, A. C.; Wilson, M. R.; Knox, C.; Bjorndahl, T. C.; Krishnamurthy, R.; Saleem, F.; Liu, P.; Dame, Z. T.; Poelzer, J.; Huynh, J.; Yallou, F. S.; Psychogios, N.; Dong, E.; Bogumil, R.; Roehring, C.; Wishart, D. S. *PLoS One* **2013**, *8*, e73076.
(24) Bar-Even, A.; Noor, E.; Flamholz, A.; Buescher, J. M.; Milo, R. *PLoS Comput. Biol.* **2011**, *7*, e1002166.
(25) Tataurova, Y.; Sealy, M. J.; Larsen, R. G.; Larsen, S. C. *J. Phys. Chem. Lett.* **2012**, *3*, 425−429.
(26) Griffiths, P. C.; Paul, A.; Hirst, N. *Chem. Soc. Rev.* **2006**, *35*, 134−145.
(27) He, Q. H.; Liu, Y. M.; Nixon, T. *J. Am. Chem. Soc.* **1998**, *120*, 1341−1342.

DOI: 10.1021/acs.analchem.5b01142
Anal. Chem. 2015, 87, 7211−7217

(28) Na, H. B.; Song, I. C.; Hyeon, T. *Adv. Mater.* **2009**, *21*, 2133−2148.
(29) Yang, X.; Stein, E. W.; Ashkenazi, S.; Wang, L. V. *Wiley Interdiscip. Rev.: Nanomed. Nanobiotechnol.* **2009**, *1*, 360−368.
(30) Bellan, L. M.; Wu, D.; Langer, R. S. *Wiley Interdiscip. Rev.: Nanomed. Nanobiotechnol.* **2011**, *3*, 229−246.
(31) De Jong, W. H.; Borm, P. J. *Int. J. Nanomed.* **2008**, *3*, 133−149.
(32) Menon, J. U.; Jadeja, P.; Tambe, P.; Vu, K.; Yuan, B.; Nguyen, K. T. *Theranostics* **2013**, *3*, 152−166.
(33) An, H.; Jin, B. *Biotechnol. Adv.* **2012**, *30*, 1721−1732.
(34) Melzak, K. A.; Sherwood, C. S.; Turner, R. F. B.; Haynes, C. A. *J. Colloid Interface Sci.* **1996**, *181*, 635−644.
(35) Arvizo, R. R.; Giri, K.; Moyano, D.; Miranda, O. R.; Madden, B.; McCormick, D. J.; Bhattacharya, R.; Rotello, V. M.; Kocher, J. P.; Mukherjee, P. *PLoS One* **2012**, *7*, e33650.
(36) del Pino, P.; Pelaz, B.; Zhang, Q.; Maffre, P.; Nienhaus, G. U.; Parak, W. J. *Mater. Horiz.* **2014**, *1*, 301−313.
(37) Cheng, L.-C.; Jiang, X.; Wang, J.; Chen, C.; Liu, R.-S. *Nanoscale* **2013**, *5*, 3547−3569.
(38) Dowding, J. M.; Das, S.; Kumar, A.; Dosani, T.; McCormack, R.; Gupta, A.; Sayle, T. X.; Sayle, D. C.; von Kalm, L.; Seal, S.; Self, W. T. *ACS Nano* **2013**, *7*, 4855−4868.
(39) Rimola, A.; Costa, D.; Sodupe, M.; Lambert, J.-F.; Ugliengo, P. *Chem. Rev.* **2013**, *113*, 4216−4313.
(40) Wishart, D. S.; Knox, C.; Guo, A. C.; Eisner, R.; Young, N.; Gautam, B.; Hau, D. D.; Psychogios, N.; Dong, E.; Bouatra, S.; Mandal, R.; Sinelnikov, I.; Xia, J.; Jia, L.; Cruz, J. A.; Lim, E.; Sobsey, C. A.; Shrivastava, S.; Huang, P.; Liu, P.; Fang, L.; Peng, J.; Fradette, R.; Cheng, D.; Tzur, D.; Clements, M.; Lewis, A.; De Souza, A.; Zuniga, A.; Dawe, M.; Xiong, Y.; Clive, D.; Greiner, R.; Nazyrova, A.; Shaykhutdinov, R.; Li, L.; Vogel, H. J.; Forsythe, I. *Nucleic Acids Res.* **2009**, *37*, D603−D610.

DOI: 10.1021/acs.analchem.5b01142
Anal. Chem. 2015, 87, 7211−7217